GODDARD
GRANT
IN-46-CR
302686
P-20

Numerical Solution of the Geoelectrodynamic Problem

Progress Report

September 6, 1990

Joseph C. Cain
Department of Geology
Florida State University
Tallahassee FL 32306

Supported by NASA Grant

NAG 5 1070

(NASA-CR-186941) NUMERICAL SOLUTION OF THE GEOELECTRODYNAMIC PROBLEM Progress Report (Florida State Univ.) 20 p CSCL 08G

N91-13813

Unclas
G3/46 0302686

Table of Contents

Introduction

The primary goal of this project is to understand the sources of the near-Earth ambient magnetic field as observed by recent spacecraft surveys and surface variational magnetic observations so as to determine (as well as the data allow) the electrical properties of the crust and upper mantle. Also included in the study is the structure and changes on a short time scale of the core field which must be separated and identified in order to achieve the pirmary goal.

The Magsat data collection interval (Nov 1979- April 1980) provides an opportunity to compare the vector field projections of ionospheric currents computed from surface data above the ionosphere as does the POGO data (1965-1971) for scalar projections. The limitation of Magsat is its sun-synchronous orbit, which only sampled low latitudes at dawn and dusk, whereas POGO, though only making observations of the scalar field, sampled all local times. Magsat operated at a lower altitude than POGO (down to 350 km) whereas the orbits of the three POGO spacecraft ranged up to 1500 km and were never lower than about 400 km.

The planned program of this study is proceeding in parallel along several lines:

1. Obtain the spherical harmonic coefficients needed to interpolate observatory hourly values. This is initially being done using observatory data taken during the 12 month interval July 1, 1979 through June 30, 1980 to span the Magsat data collection interval. Earlier data, taken during the POGO data collection (1965-1971) have also been used and will be part of the analysis following the Magsat work. The intent is to produce a set of hourly coefficients for the interval from about 1960 through 1980 for these and future studies.

2. Obtain an accurate high degree model of the static field so as to be able to compare the projected results from (1) with the deviations from Magsat to investigate how these potential expressions portray the field variations above the ionosphere. (We already know of deviations due to meridional and field aligned currents and plan to add the appropriate non-potential functions to allow their modelling.) Study and understand the ionospheric/magnetospheric interactions as are appropriate to observatory, Magsat and POGO data sets.

3. Develop functions that will relate the external variations imposed on the Earth to its electrical response.

4. Invert the results of the internal/external relations to determine physically meaningful conductivity models of the crust and upper mantle.

5. Study the short period secular variation determined from the interval 1960-1980 in regard to such topics as frozen flux and energy transfer as may be pertinent to a fuller understanding of the physics of the core dynamo. This requires separation of apparent core secular variation due to long term changes of externally imposed flux from that arising in the core.

6. Look for the physical bases for the crustal signals for the range n = 14 - 50; whether they can be explained completely in terms of crustal magnetization. Our speculation is that there is the possibility that potentials driving weak currents through conductivity channels in the crust and upper mantle may be contributing to the crustal signatures.

Data

The observatory data being used is indicated in Table 1. These are the data for which a complete year are available (July 1, 1979- June 30, 1980), and in hand. In addition to this set, there are others for which a partial year is available or more that has been found recently but not yet acquired or processed. These are noted in table 2.

There are a number of stations for which there should be data, because they were collected by this project or entered onto the data base from printed listings. The reductions were only being done for data from September, 1979 through June of 1980. These had been turned over to the data center in 1985 or 1986. It is thus unclear and subject to further investigation as to what happened to the data sent to them at that time. Figure 1 shows the locations of these stations.

Table 1: Magnetic observatories for which a full year's data (July 1, 1979- June 30, 1980) are in hand and either adjusted if discontinuities, or otherwise processed into an analytic format. (Most of these can be identified by reference to several listings provided by the World Data Centers for Geomagnetism or in such references as *Langel* (1987)).

AIA	GWC	MNK
AMT	HER	NUR
AQU	HON	NEW
BNG	IRT	NVS
BOU	KAK	PMG
BRW	KGL	SGE
CBB	LOV	SIT
CMO	LRV	SJG
CNB	MBC	STJ
CZT	MEA	TUC
FCC	MMB	VIC
GUA		WIT
		YKC

Table 2 Data which are available from sources other than the World Data centers or which are received but not yet validated or entered into the analytic base. Those in parentheses are available from other sources and are reported to have been validated, those in square brackets are not yet received and are in some raw form. The numbers following the brackets indicate the year and the number of element months reported to be available for that year.

[ALE 79: 30]
BLC 79
BJI 80
BLC 80 [BLC 79:33]
CAN 80 [CAN 79:12]
CNH 80
GNA 79 [GNA 80:18]
DRV 80 [DRV 79:43]
[ebr 79:2]
ESK 80
FRD 80 (FRD 79)
[FUR 79:11, 80:10]
GNA 80
GZH 80
HAD 80 (HAD 79)
HRB 80
HUA 80 [HUA 79:12]
ISK 80
JAI 80
KGD 80
(KNY 80) KNY [79:36]
(LER)
MBO 80 [MBO 79:12]
MIR 80
MIZ 80
(MOS 79)
MMK 80 [MMK 79:36]
LMM 80
LNP 80
LZH 80
(NGK 80)
NKK 80
ODE 80
OTT 80 [OTT 79:8]
POD 80
PPT 80 [PPT 79:12]
RES 80 [RES 79:8]
RSV 80
SNA 80
SOD 80
SSH 80
SVD 80 [SVD 79:35]
TKT 80
TOL 80 [TOL 79:12]
[TOO 79:18]
TRD 80
(VLA 79) [VLA 80:36]
VSS 80 [VSS 79:12]
WHN 80
WHS 80 [WHS 79:4]
(YAK 79)

OBSERVATORY DISTRIBUTION

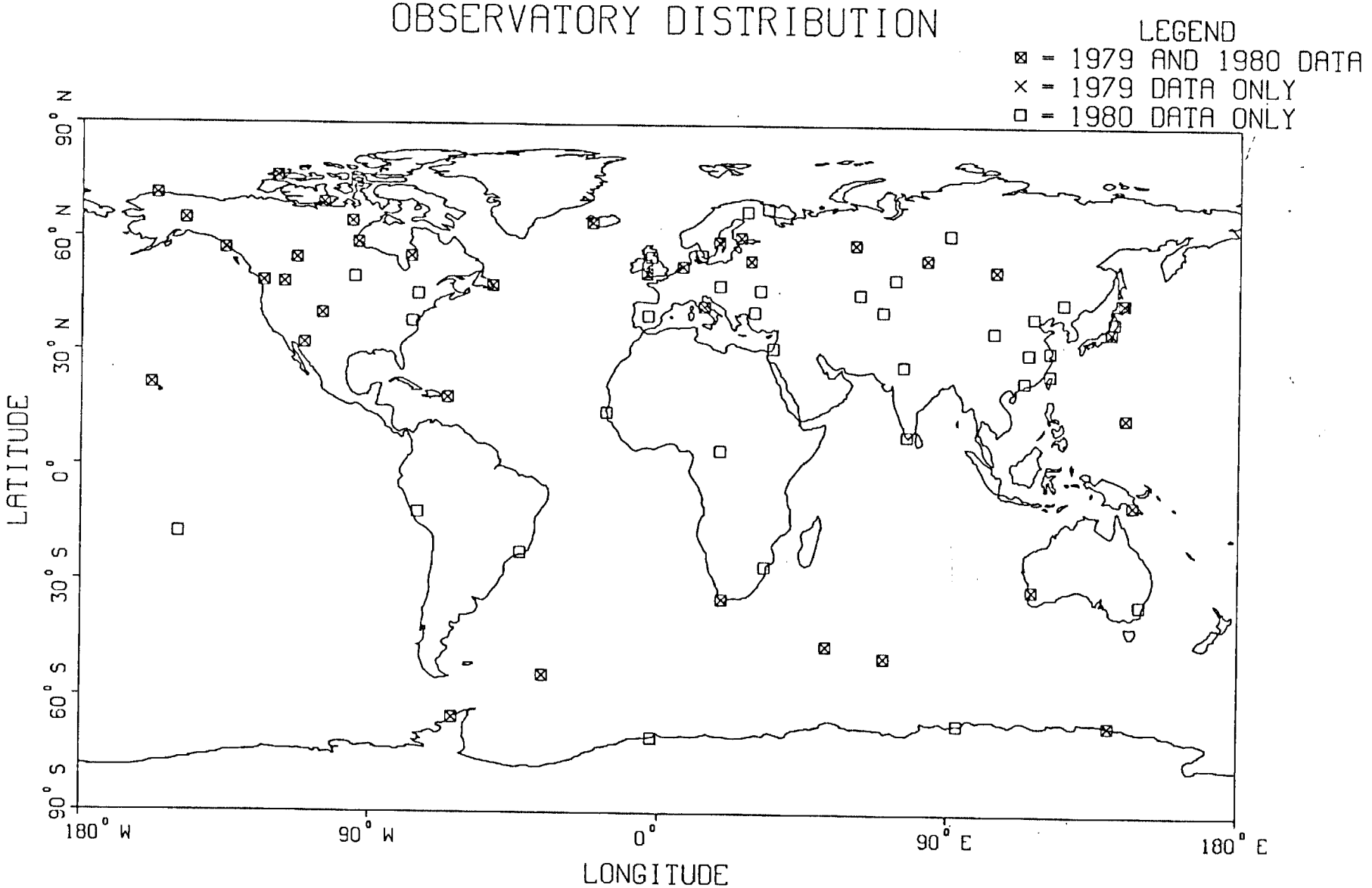

Theory

The classical method of representing diurnal variations of observatory hourly data has been to compute an equivalent sheet current system at about 100 km altitude expanding the potential function of the observed variations in low degree spherical harmonics (*Chapman*, 1919). This technique has been applied mainly to averages taken over quiet intervals after removing a base value for each station taken. Such removal implies that the equivalent electrical currents obtained are those relative to that at some local time (e.g. midnight), when such currents should be weak or non-existent. The usual coordinate system for making such computations has been latitude (or magnetic latitude) and some form of local time. A more modern look at such currents was by *Suguira* and *Hagan* (1967) who were able to compute the potential of the variations for each hour of Universal time for two selected 5-day intervals.

The potential function of the time variational field was expressed by:

$$V(r,\alpha,\lambda,T) = a \sum_{n=1}^{4} \sum_{m=1}^{n} \left[\left[g_n^{m(e)}(T) \cos m\lambda + h_n^{m(e)}(T) \sin m\lambda \right] \left[\frac{r}{a} \right]^n + \left[g_n^{m(i)}(T) \cos m\lambda + h_n^{m(i)}(T) \sin m\lambda \right] \left[\frac{a}{r} \right]^{n+1} \right] P_n^m(\cos\theta)$$

The variational field **B** is obtained from such functions by the negative gradient $\mathbf{B} = -\nabla V$.

A problem with determining the coefficients is the large gaps in spatial coverage of the data, even limiting the degree to n = 4. Past experience with such analyses has been that the least squares process would sometimes not converge, or would converge on very spurious results with too sparse a data distribution. It has often been found useful to supplement the distribution allowing the data for a given hour to enter the computation several times. One method used 3-hour running averages by considering time differences to be equivalent to longitude differences within each 3- hour interval. If the computation was done to produce values at time T, a value of the field difference for time T-1 and T+1 was also entered with longitudes -15° and +15° respectively from the longitude at time T. This is equivalent to using a box car filter with 3 point overlaps in the time domain.

Our approach here is to develop the coefficients per UT day by expansion of the time terms in the coefficients. However, difficulties in obtaining detailed results, or, in some instances, results that will converge at all, may force us to adopt similar expedients as above. Also, because data will be obtained above the presumed source of ionospheric currents as well as below, we separate out the different potentials as noted in our earlier report as follows:

$$V = V_c^i + V_s^e + V_s^i + V_m^e$$

where the potentials are identified with the following sources:

V_c^i : core field

V_s^e : E/F layer ionospheric currents

V_s^i : Internal Earth currents induced by external flux changes

V_m^e : Magnetospheric currents external to the spacecraft shell as well as the Earth

For our purposes here we expand the coefficients of the internal field into linear time derivatives so as to take into account secular variation only over a short period. This expression is thus:

$$V_c^i = a \sum_{n=1}^{n_c} \left(\frac{a}{r}\right)^{n+1} \sum_{m=0}^{n} \left\{ \left[g_n^m + \dot{g}_n^m (\delta t) \right] \cos m\phi + \left[h_n^m + \dot{h}_n^m (\delta t) \right] \sin m\phi \right\} P_n^m (\theta)$$

The present limit to n_c is 50 for the spatial terms and 7 for the first time derivatives (SV) as determined for the Magsat interval. This is the most recent model determined using least squares only for the high degree terms and will be published soon (*Cain et al.* 1990). The secular change terms are those derived by *Cain et al.* (1989a) using a combination of observatory secular change and Magsat. This SV is not adequate and will need to be revised after the external field computation is complete because it is likely that some of the seasonal changes from ionospheric currents and their induced analogs are incorporated in the first time derivatives.

The form of the V_m^e terms is:

$$V_m^e = r \left\{ g_1^{0e} \cos\theta + \left[g_1^{1e} \cos\phi + h_1^{1e} \sin\phi \right] \sin\theta \right\}$$

The potential for the currents induced in the Earth from the changes in all external currents, both ionospheric and magnetospheric, is:

$$V_s^i = a \sum_{n=1}^{n_v} \left(\frac{a}{r}\right)^{(n+1)} \sum_{m=0}^{n} \left[G_n^{mi} \cos m\phi + H_n^{mi} \sin m\theta \right]$$

and for the ionospheric currents themselves:

$$V_s^e = a \sum_{n=1}^{n_v} \left(\frac{r}{a}\right)^{n} \sum_{m=0}^{n} \left[G_n^{me} \cos m\phi + H_n^{me} \sin m\phi \right]$$

where the terms for G_n^{me} and H_n^{me} are:

$$G_n^{me} = \sum_{j=1}^{n} \left(\alpha_{nj}^{me} \cos jt + \beta_{nj}^{me} \sin jt \right)$$

$$H_n^{me} = \sum_{j=1}^{n} \left(\gamma_{nj}^{me} \cos jt + \delta_{nj}^{me} \sin jt \right)$$

with expressions for the internal functions corresponding to these by replacing "e" by "i."

The above are for computations below the ionosphere (i.e. at the Earth's surface). However, above the ionosphere, the potential for the ionospheric currents changes so that, for a continuous vertical field across the sheet, the potential becomes an internal one:

$$Q_s^i = -a \sum_{n=1}^{n_v} \left(\frac{R}{a} \right)^{(2n+1)} \left(\frac{n}{n+1} \right) \left(\frac{a}{r} \right)^{(n+1)} \sum_{m=0}^{m} \left[G_n^{me} \cos m\phi + H_n^{me} \sin m\phi \right]$$

It is clear that there is no way from surface data to distinguish the n = 1 terms from the ring current from an n = 1 term from the ionosphere. Thus for the determinations prior to addition of satellite data, the adjustment for the potential V_m^e is being turned off and left entirely to the potential V_s^e. (Most other workers have ignored this term).

For our studies we will make no selection of data for quiet, but instead compute the potential for all UT hours under consideration. Although the field aligned currents and the near equatorial meridional currents (*Yanagasawa* and *Kono*, 1985; *Cain et. al.*, 1989) are not yet added to the fitting functions, most of these effects are non-potential and are ignored initially. A reason why it is valid initially to ignore these currents is that the vertical component are non-potential and thus do not affect the potential function being developed. Their horizontal components will be potential, and will vary with altitude and affect the Magsat data especially. In polar regions the field aligned currents are near vertical and most of the main field analysis has used data when they were very weak. Recent work by *Langel, Rajaram,* and *Purucker* (1990) on the structure of the meridional currents near the dusk equator will be helpful in further modeling for these currents.

Potential field testing

As a means of testing this program, some of the previously reduced data during the POGO interval were used. Data were from 34 magnetic observatories for the period Sept 22 - 27, 1967. By using the expedient of computing the variational potentials from the rediduals of the data from the average night-time values (21 - 2 hours local time), the coefficients were obtained as seen in Table 3. These appear to have about the correct amplitudes compared with those of *Sugiura* and *Hagan* (1967) (after converting theirs to Schmidt normalization). This can be especially seen in the large diurnal term for the n = 2, m = 1 external coefficents.

Table 3a

Sample coefficients for external potential functions averaged over 6 days in September 1967. See equations

j	n	m	α	β	γ	δ
1	1	0	.383	2.300		
1	1	1	1.15	-2.059	-1.553	-.251
1	2	0	.455	-2.482		
1	2	1	7.643	-.829	-1.25	-7.85
1	2	2	.105	-2.497	-2.994	.870
1	3	0	-1.796	1.157		
1	3	1	-1.059	1.285	.653	2.621
1	3	2	-.635	-.833	1.51	.552
1	3	3	-1.685	-.068	-.753	-1.549
2	1	0	-1.256	.663		
2	1	1	-.185	-.602	-.853	-.946
2	2	0	-.344	1.060		
2	2	1	-.160	.267	1.472	.688
2	2	2	.781	2.592	3.648	-.257
2	3	0	.628	.654		
2	3	1	-1.090	1.014	-.320	.221
2	3	2	-.524	.568	-.159	4.037
2	3	3	-.567	.218	.652	.413
3	1	0	.701	-.7365		
3	1	1	-1.496	-.774	-.977	1.056
3	2	0	.393	.320		
3	2	1	.508	.597	.992	.126
3	2	2	-.822	1.401	.440	.240
3	3	0	.434	.425		
3	3	1	.166	-.832	-.810	-.134
3	3	2	.829	-.110	-.192	-.734
3	3	3	-.212	-1.845	-1.65	.559

Table 3b

Sample coefficients for internal potential functions averaged over 6 days in September 1967. See equations.

j	n	m	α	β	γ	δ
1	1	0	1.638	.093		
1	1	1	-.308	-.571	-1.658	-1.607
1	2	0	-.499	-.531		
1	2	1	3.244	.424	-1.137	-1.468
1	2	2	-.009	-4.38	.034	.374
1	3	0	.415	-.014		
1	3	1	1.254	2.078	1.046	-1.125
1	3	2	.767	-.315	.337	.164
1	3	3	-.459	-.404	.265	-.841
2	1	0	1.297	.548		
2	1	1	1.132	-.451	-.031	.271
2	2	0	-.657	.010		
2	2	1	-1.186	1.181	-.824	.059
2	2	2	.169	.437	.539	-.098
2	3	0	.224	.238		
2	3	1	.572	-.358	.193	-.388
2	3	2	-1.044	.853	.618	1.592
2	3	3	-.058	.396	-.808	-.019
3	1	0	.161	-.803		
3	1	1	-1.133	.166	.566	.433
3	2	0	-.028	.012		
3	2	1	.076	-.205	-.087	.195
3	2	2	-.304	-.631	.629	-.011
3	3	0	.145	.004		
3	3	1	.557	-.397	.110	.210
3	3	2	-.160	-.014	-.398	-.730
3	3	3	-.053	.179	-1.065	.736

Another way to view such results is to look at maps of either the current function or the potential function. The two functions are similar. As noted earlier, the potential above and below the assumed ionospheric current sheet are different and can be also expressed in terms of the potential of a surface current as follows:

$$V = -R\sum_{n=1}^{\infty} n\left(\frac{R}{r}\right)^{n+1} S_n, \quad for \quad r\rangle R \quad or$$

$$R\sum_{n=1}^{\infty} (n+1)\left(\frac{r}{R}\right)^{n} S_n, \quad for \quad r\langle R$$

where S is:

$$S_n = \sum_{m=0}^{n} \left[\zeta_n^m \cos m\phi + \eta_n^m \sin m\phi\right]$$

The current density J of such an ionospheric sheet can be shown (within an arbitary constant) to have components in the south and east directions respectively of:

$$J_\theta = -\frac{5}{2\pi}\sum_{n=1}^{\infty}\left[\frac{2n+1}{\sin\theta}\right]\frac{\partial S_n}{\partial\phi}$$

$$J_\phi = \frac{5}{2\pi}\sum_{n=1}^{\infty}(2n+1)\frac{\partial S_n}{\partial\theta}$$

The potentials for V_s^e can then be matched up to those for S_n with the result that the contours of J and of V_s^e are parallel. We here plot the potentials of $V_s = V_s^e + V_s^i$ in order to visualize whether the program is producing reasonable patterns to also correspond in structure to those of equivalent ionospheric current systems. That is, the current direction is indicated by that of the contours and the current density by the crowding of the contours.

Figure 2 is a representation of the contours of the sum of the potentials V_s for 4 different universal times. There is clearly some problem with a discontinuity on the prime meridian due likely to the method of analysis. Otherwise, the cellular structure is not dissimilar from those plotted previously. In general the strongest currents are near the noon meridian with the northern focus earlier in time than the southern.

However, there are sufficient differences from prior current patterns to make it imperative that these computations be scrutinized in detail and further tests made using synthetically produced data to assure

that all programs are producing accurate results. Also, instead of attempting to validate the POGO data that went into this computation, which would require re-acquiring surface data for this interval, we plan instead to first concentrate on the Magsat interval.

Internal/External Relations

The development of a connecting matrix to express the response of the Earth to an imposed external field was developed by a prior NASA contract (NAS 5-9319) but never implemented completely due to the complexity of the functions required and the limitations of computing equipment at that time. The development that follows is thus an outline of the technique that might be a useful tool for analysis simultaneously to providing the basic functions needed to determine the Earth's internal conductivity structure.

The premise was that there exists an impedance function $z(\theta,\phi,\omega)$ that relates the tangential electric field **E** and surface current density by the equation $\mathbf{E} = z\, J_{tan}$. That is, the solid Earth would be represented by a thin shell. The usefulness of such a function becomes apparent especially when one looks at the power spectrum of the diurnal variations (e.g. *Parkinson*, 1983, P. 261). These show that the major power is in harmonics and subharmonics of the diurnal period. Also, luni-solar harmonics are imposed from the lunar tidal terms interacting with the changing electron density.

Thus it may be practicable to determine such a shell function at specific frequencies which represent most of the power in the quiet diurnal field patterns. There is some evidence that the disturbance field may also be so broken up into a small number of discrete frequencies. However, the theory does not require that a small number be used, and there may be ways of obtaining band passed averages if the spectrum does not have sharp peaks as it does during quiet conditions.

It can be shown that if

$$a = R\sum_{n=1}^{\infty} (2n+1)\ S_{in\,n}$$

$$b = -R\sum_{n=1}^{\infty} n(n+1)\,(2n+1)\,S_{in\,n}$$

$$c = \mu_0\sum_{n=1}^{\infty} n(n=1)\left(\dot{S}_{ez\,n} + \dot{S}_{in\,n}\right)$$

equations can be set up of the type

$$\nabla a \bullet \nabla z + bz = c$$

which should yield two real functions for each frequency given the proper variational input to be able to produce current functions of the type S_n as expressed earlier.

POTENTIAL OF GEOMAGNETIC VARIATIONS

6 UT

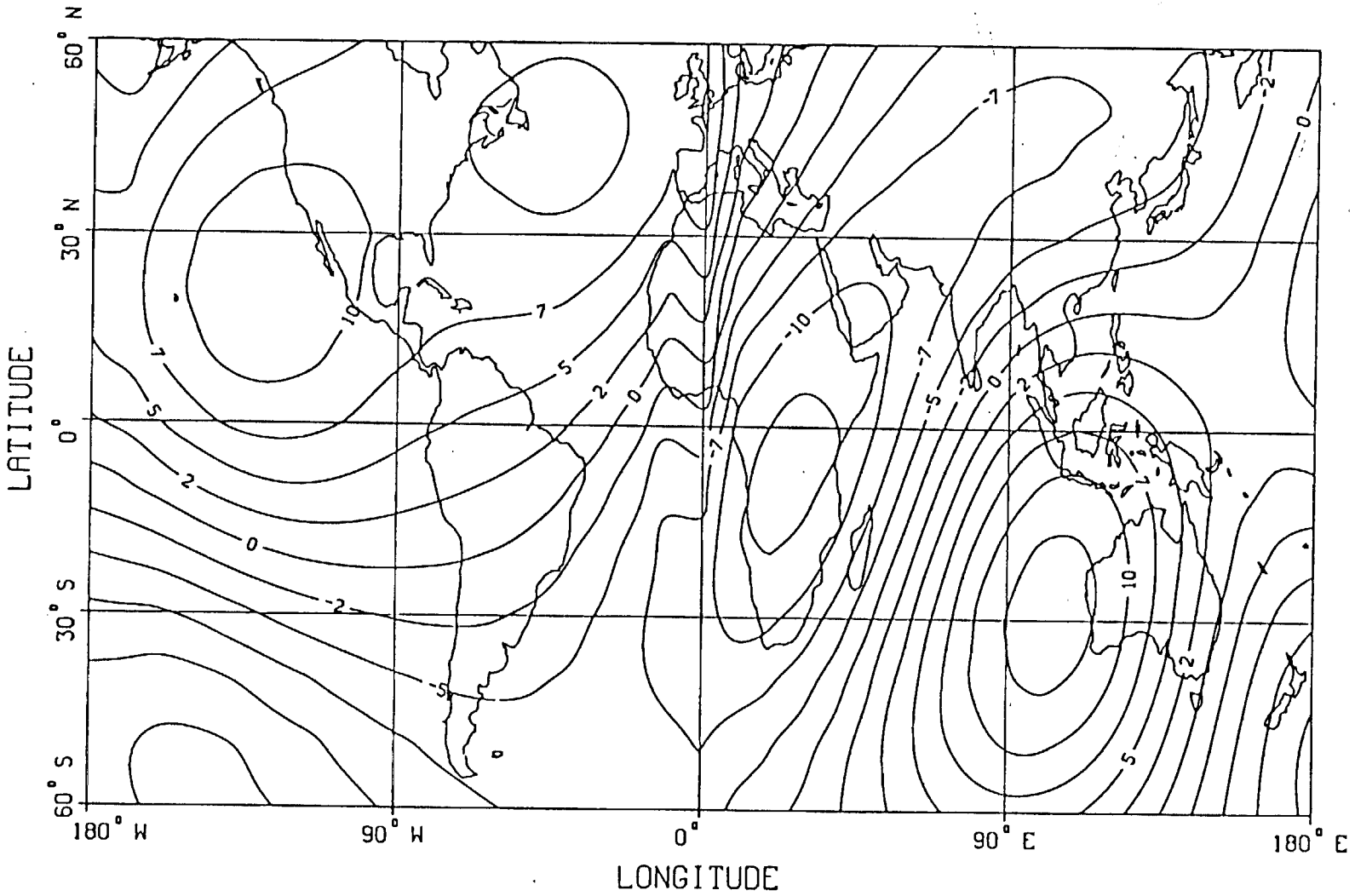

POTENTIAL OF GEOMAGNETIC VARIATIONS

12 UT

Average for 5 days during OGO-2/4 data collection (Sept 1967) Quiet magnetic conditions

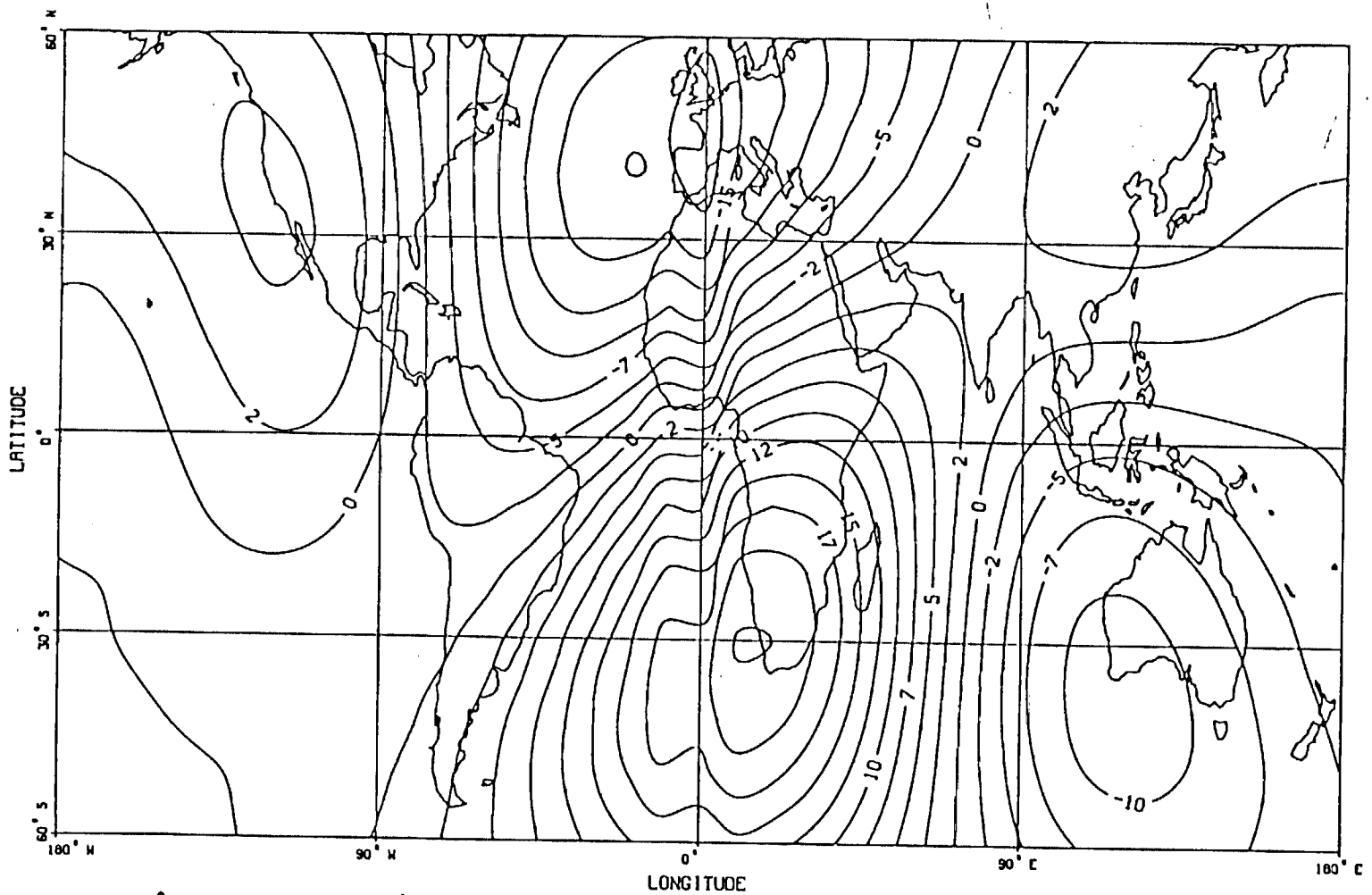

initial plot of function $V(r, \theta, \varphi, t) = V_i + V_e$ for $r = a$ (surface)

(Discontinuity due to error in smoothing function)

POTENTIAL OF GEOMAGNETIC VARIATIONS

18 UT

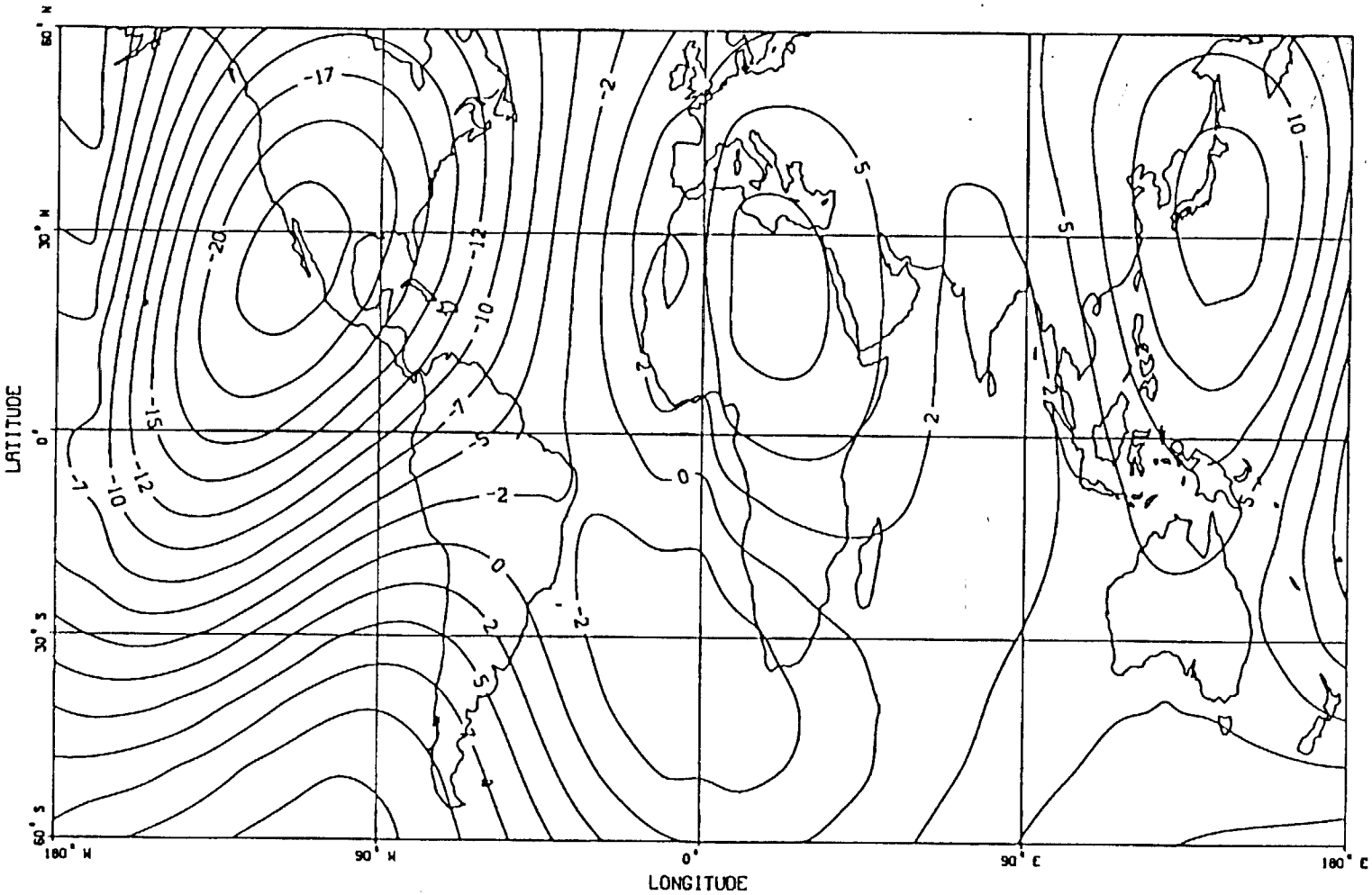

POTENTIAL OF GEOMAGNETIC VARIATIONS

24 UT

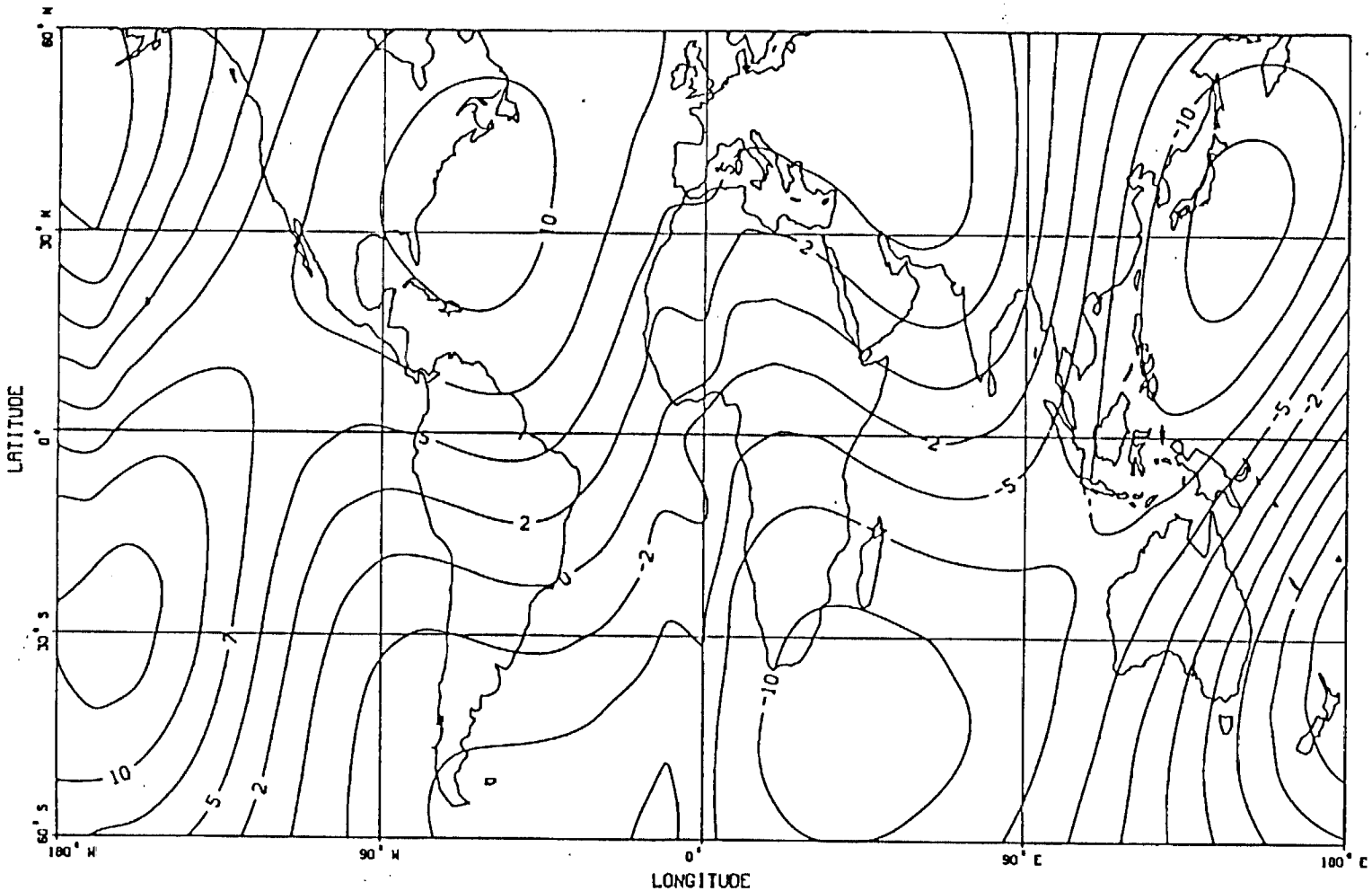

Crustal Field

The high degree field model from Magsat and surface observatory secular change data was initially developed by a series of papers now in print (*Cain et al.* 1989a,b). This model was recently tested under this project and found to have questionable error distributions so was recalculated with adjustments to n = 50. This paper is to be published in September and a copy is attached herein. Also included in this copy are some added error distributions that did not appear in the printer version of the paper.

It is not completely certain why the integral method applied to the Z component for obtaining the coefficients to n = 63 gave such poor results. Our supposition at this time is that it was due to the fact that the field above the ionosphere was seriously affected by the external currents. It was noted in the development of the model for correction of the "ionospheric currents" (*Cain* 1989a) that the residuals were not uniform as to epoch and altitude. There were systematic biases depending on how the data were selected. However, due to the need to obtain results with less than adequate resources, we were unable to pursue these questions in detail. It would seem that the new model is adequate to use as a base for comparing the results of the surface model projected ionospheric current changes to satellite altitude.

Future plans

In the last progress report it was noted that we were faced with considerable uncertainty as our supercomputer company (ETA) had suddenly gone out of business. At this time we have now converted to an operational Cray YMP and also have an added Connection Machine 2. Our Sun workstation has also had its memory expanded to 24 mbytes and disk expanded to 900 mbytes. Thus such problems are now essentially behind us.

Validating and completing the observatory hourly value set for the Magsat interval is high on the priority list. This will require more detailed looking at the baselines and comparing with averages computed by *Cain* and *Kluth* (1984, 1985).

The procedure of computing the external and internal field variations from surface and satellite data needs to be rechecked using synthetic data.

Further work needs to be done on the theory of relating internal and external source functions.

References

Chapman, S., The solar and lunar diurnal variation fo the Earth's magnetism, *Phil. Trans. Roy. Soc. London, A*, **218**, 1-118, 1919.

Cain, J. C., D. R. Schmitz, and C. Kluth, Development of an improved Magsat internal field model, *EOS*, **65**, 871, 1984.

Cain, J. C. and C. Kluth, An evaluation of the 1985-1990 secular variation candidates, *Phys. Earth and Planet. Inter.*, **48**, 362-378, 1985.

Cain, J. C., Z. Wang, C. Kluth, and D. R. Schmitz, Derivation of a Geomagnetic Model to n = 63, *Geophysical Journal*, **97**, 431-441, 1989a.

Cain, J. C., Z. Wang, D. R. Schmitz and J. Meyer, The geomagnetic spectrum for 1980 and core-crustal separation, *Geophysical Journal*, **97**, 443-447, 1989b.

Langel, R. A., The main field, pp 249-512 in **Geomagnetism** Vol 1, J. A. Jacobs (ed), Academic Press, 1987.

Langel, R. A., M. Rajaram, and M. Purucker, The equatorial electrojet and associated currents as seen in Magsat data, (personal communication), 1990.

Parkinson, W. D., Introduction to Geomagnetism, Elsevier, 1983.

Schmitz, D. R., J. Meyer, and J. C. Cain, Modeling the Earth's geomagnetic field to high degree and order, *Geophysical Journal*, **97**, 421-430, 1989.

Sugiura, M. and M. P. Hagan, Universal-time changes in the geomagnetic solar quiet daily variation Sq and A study of seasonal changes in the geomagnetic Sq variation by a motion picture representation, NSF Report GA-478, Department of Atmospheric Sciences, Univ. Washington, 1967.

Yanagasawa, M. and M. Kono, Mean ionospheric field correction for Magsat data, *J. Geophys. Res.*, **90**, 2527-2536, 1985.

Appendix A - Numerical Experiments in Geomagnetic field modelling

J. C. Cain, B. Holter, and D. Sandee

Journal of Geomagnetism and Geoelectricity, **42**, 961-972, 1990.

This is the version as submitted to the above Journal. Several small errors were corrected in the final version which is not yet available.